ACS chemical biology

Letters

Cite This: ACS Chem. Biol. XXXX, XXX, XXX−XXX

pubs.acs.org/acschemicalbiology

Combining Chemical Genetics with Proximity-Dependent Labeling Reveals Cellular Targets of Poly(ADP-ribose) Polymerase 14 (PARP14)

Ian Carter-O'Connell,*[,†,§] Anke Vermehren-Schmaedick,[†] Haihong Jin,[†] Rory K. Morgan,[†] Larry L. David,[‡] and Michael S. Cohen*[,†]

[†]Program in Chemical Biology and Department of Physiology and Pharmacology, Oregon Health and Science University, Portland, Oregon 97210, United States

[‡]Department of Biochemistry, Oregon Health and Science University, Portland, Oregon 97210, United States

Supporting Information

ABSTRACT: Poly(ADP-ribose) polymerase 14 (PARP14) is a member of the PARP family of enzymes that transfer ADP-ribose from NAD$^+$ to nucleophilic amino acids on target proteins, a process known as mono-ADP-ribosylation (MARylation). PARP14 is involved in normal immune function through the IL-4 signaling pathway and is a prosurvival factor in multiple myeloma and hepatocellular carcinoma. A mechanistic understanding of the physiological and pathophysiological roles of PARP14 has been limited by the dearth of PARP14-specific MARylation targets. Herein we engineered a PARP14 variant that uses an NAD$^+$ analog that is orthogonal to wild-type PARPs for identifying PARP14-specific MARylation targets. Combining this chemical genetics approach with a BioID approach for proximity-dependent labeling of PARP14 interactors, we identified 114 PARP14-specific protein substrates, several of which are RNA regulatory proteins. One of these targets is PARP13, a protein known to play a role in regulating RNA stability. PARP14 MARylates PARP13 on several acidic amino acids. This study not only reveals crosstalk among PARP family members but also highlights the advantage of using disparate approaches for identifying the direct targets of individual PARP family members.

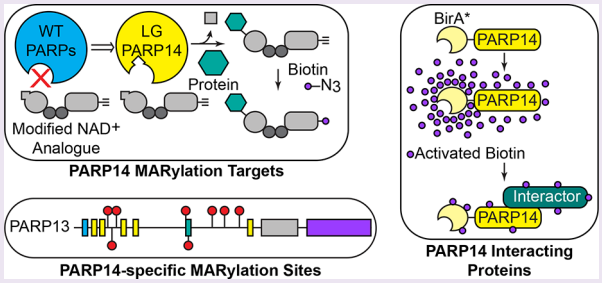

Poly(ADP-ribose) polymerase 14 (PARP14, ARTD8, or BAL2) is a member of the PARP family of enzymes (17 in humans) that have emerged as important factors in cell signal transduction[1] and are implicated in a host of physiological[2−4] and pathophysiological[5] pathways. PARPs contain a conserved catalytic domain that transfers ADP-ribose from nicotinamide adenine dinucleotide (NAD$^+$) onto their protein targets.[6] The PARP family can be divided between PARP enzymes that transfer a single ADP-ribose moiety (e.g., PARP14)[7] and those that transfer multiple ADP-ribose moieties (e.g., PARP1).[8] Mono-ADP-ribosylation (MARylation) is sufficient to dramatically alter enzyme function: disrupting protein−protein interactions, inhibiting enzyme function, and creating new surfaces for binding.[6,9]

PARP14 plays an important role in normal immune function where it regulates interleukin-4 (IL-4) and signal transducer and activator of transcription 6 (STAT6)-dependent transcription in T and B cells.[10−12] Further, it was shown to regulate interferon beta (IFN-β) in macrophages.[13] Beyond its role in normal immune function, PARP14 was shown to play an antiapoptotic role in both multiple myeloma (MM)[14] and hepatocellular carcinoma (HCC).[15] While the activity of PARP14 is required for its role in gene regulation in immune cells and in cancer cell survival, the direct MARylation targets of PARP14 are unknown. Without this information, it has been difficult to determine the mechanism by which PARP14-mediated MARylation regulates these processes.

Recently, our lab and others have developed a chemical genetic strategy using engineered PARP−modified NAD$^+$ analog pairs for identifying the direct targets of PARP family members.[16−19] Herein, we report the expansion of our chemical genetic strategy for identifying the direct targets of PARP14. By engineering a variant of PARP14 that is able to use a modified NAD$^+$ analog, we identified 114 PARP14-specific MARylation targets. The PARP14 targets we identified are significantly enriched for RNA regulatory proteins and proteins involved in translation initiation, elucidating a broad role for PARP14 in post-transcriptional regulation. We discovered that PARP13, an inactive PARP family member that regulates RNA stability, is a *bona fide* PARP14 target, demonstrating crosstalk among PARP family members. Using a combined higher-energy collisional dissociation (HCD) and electron-transfer dissociation (ETD) LC-MS/MS method,[20] we identified 8 novel PARP14-specific MARylation sites on

Received: June 19, 2018
Accepted: September 24, 2018
Published: September 24, 2018

DOI: 10.1021/acschembio.8b00567
ACS Chem. Biol. XXXX, XXX, XXX−XXX

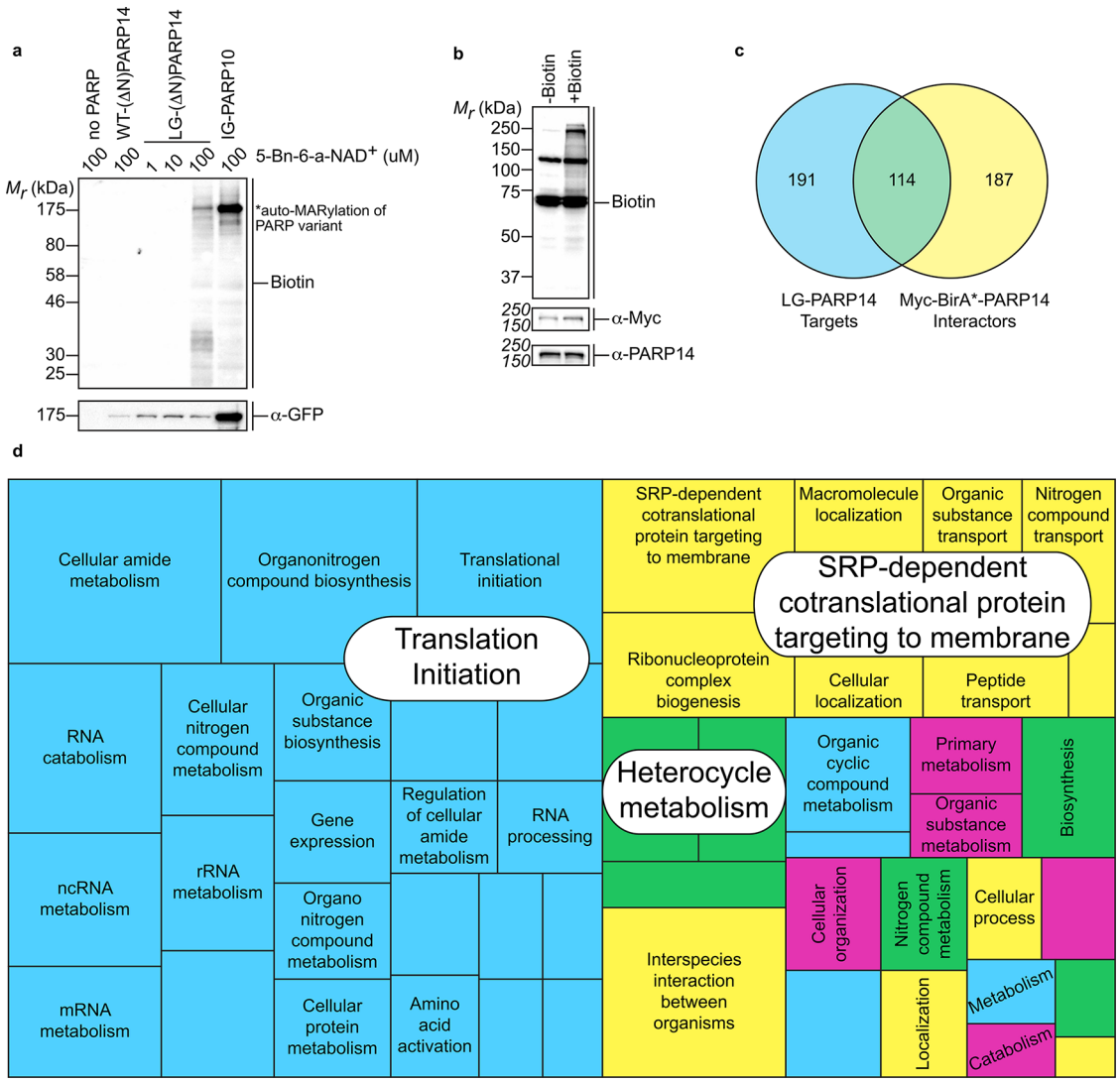

Figure 1. Identification of PARP14 targets using a chemical genetic and "interactor" biotin affinity capture approach. (a) Lysate labeling by WT-ΔN-PARP14, LG-ΔN-PARP14, and IG-PARP10 in the presence of 5-Bn-6-a-NAD$^+$. HEK 293T cells were transfected with either WT-ΔN-PARP14, LG-ΔN-PARP14, or IG-PARP10 and subjected to lysate labeling for 2 h in the presence of varying amounts of 5-Bn-6-a-NAD$^+$. MARylated proteins were visualized using streptavidin−HRP (Biotin). Expression of each PARP variant was confirmed via immunoblot detection of GFP. (b) Biotinylation of proximal PARP14 "interactors" by Myc-BirA*−PARP14 in the presence of biotin. HEK 293T cells were transfected with Myc-BirA*−PARP14 and treated with media supplemented with vehicle (−Biotin) or biotin (+Biotin) for 24 h. Biotinylated proteins were visualized using streptavidin−HRP (Biotin). Expression of Myc-BirA*−PARP14 was confirmed via immunoblot detection of Myc and PARP14. (c) Venn diagram comparing the LG-PARP14 targets identified in at least one LC-MS/MS run and the PARP14 "interactors" identified using Myc-BirA*−PARP14. (d) Tree map depicting enriched GO terms attached to the 114 shared LG-PARP14 and Myc-BirA*−PARP14 targets. GO term enrichment was performed using the PANTHER toolkit. Significantly enriched GO terms ($p < 0.05$) were condensed using ReviGO and similar terms were nested based on similarity. Selected terms are indicated. The area of each box is proportionally scaled to the $-\log_{10}(p\text{-value})$.

PARP13. These sites display differential PARP14-dependent MARylation rates, and their mutation to alanine resulted in a significant decrease in PARP14-dependent labeling.

We have previously developed engineered PARP−modified NAD$^+$ analog pairs for identifying PARP family member specific protein targets within complex cellular lysates.[16−18] Our method relies on the introduction of a novel hydrophobic pocket near the active site of the specific mono-PARP that will accommodate a modified NAD$^+$ analog. 5-Benzyl-6-alkyne-NAD$^+$ (5-Bn-6-a-NAD$^+$) has a benzyl substituent at the C-5 position of the nicotinamide ring that allows it to be exclusively used by an engineered mono-PARP. The modification of NAD$^+$ at this position prevents endogenous PARPs from using 5-Bn-6-a-NAD$^+$ as a substrate. The N-6 position of the adenosine ring contains an alkyne tag for enrichment of MARylated protein targets using "click" chemistry and subsequent identification of them using LC-MS/MS.

Based on the primary sequence of PARP14, we hypothesized that mutation of Leu1782 to a glycine would confer sensitivity to 5-Bn-6-a-NAD$^+$. Initially, we introduced this mutation into a variant of PARP14 that is lacking the first 553 amino acids of the N-terminus (ΔN-PARP14). We started with this construct because it lacks a region that will recombine in most *E. coli* strains (with the exception of NEB stable cells grown at RT) making it easier to manipulate. We expressed the engineered form of PARP14 (LG-ΔN-PARP14) in HEK 293T cells and incubated the lysates with increasing concentrations of 5-Bn-6-a-NAD$^+$. In lysates from cells transfected with LG-ΔN-

DOI: 10.1021/acschembio.8b00567
ACS Chem. Biol. XXXX, XXX, XXX−XXX

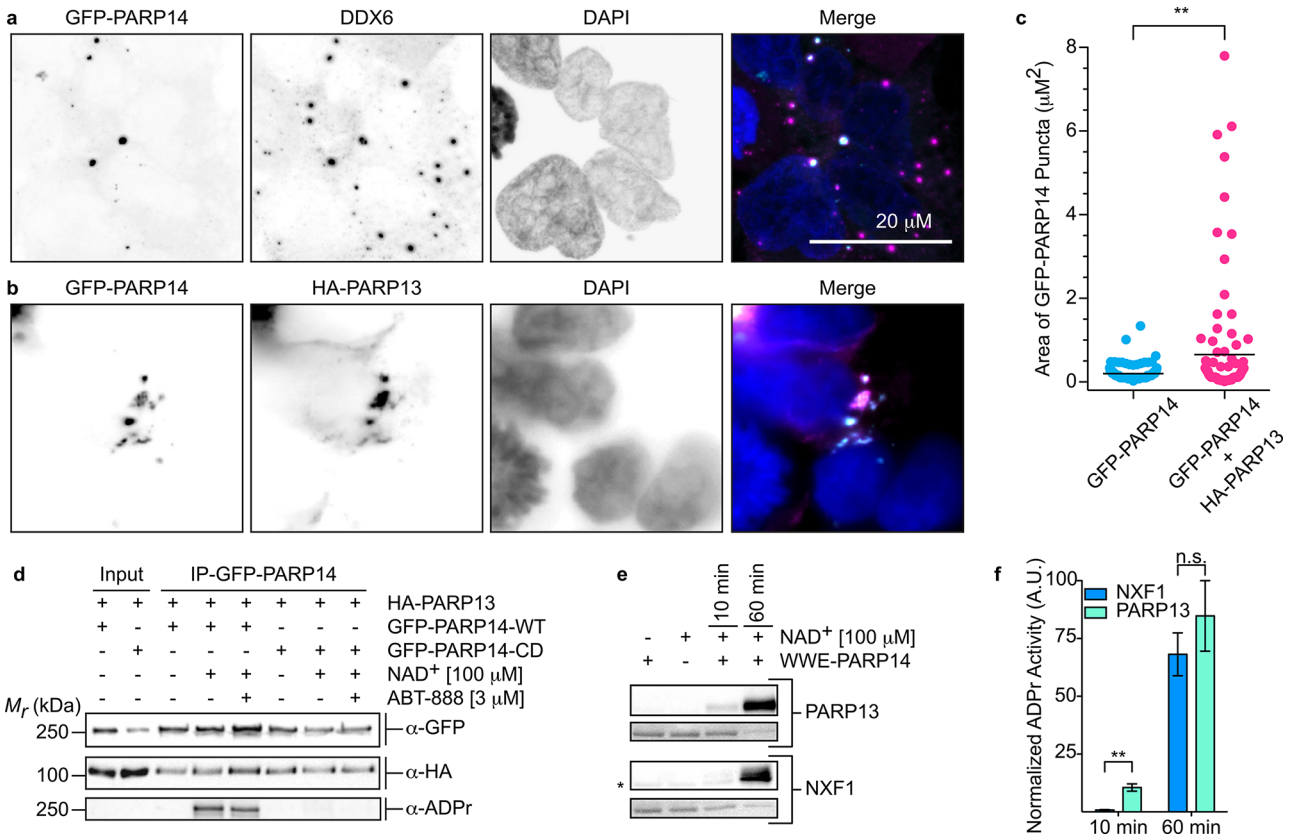

Figure 2. PARP14 colocalizes with RNA regulatory proteins in the cell and modifies PARP13 *in vitro*. (a) GFP−PARP14 and DDX6 are colocalized in cytoplasmic puncta. HEK 293T cells expressing GFP−PARP14 were fixed with paraformaldehyde and processed for immunofluorescence. DNA was stained with DAPI. Scale bar = 20 μM. (b) GFP−PARP14 and HA−PARP13 are colocalized in cytoplasmic puncta. Cells were treated as described in part a. (c) HA−PARP13 coexpression increases the surface area of GFP−PARP14 puncta. The surface area of GFP−PARP14 puncta from HEK 293T cells expressing GFP−PARP14 alone (n = 104) or GFP−PARP14 and HA−PARP13 (n = 99) is depicted as a scatter plot, and the mean is indicated. ** represents p-value < 0.01, two-tailed Student's t test. (d) HA−PARP13 coprecipitates with GFP−PARP14. HEK 293T cells expressing HA−PARP13 and either GFP−PARP14-WT or GFP−PARP14-CD were lysed and affinity purified using the GFP tag. Lysates were treated with NAD^+ or ABT-888, and PARP13 and PARP14 were detected via immunoblot. MARylation was detected using MABE1016 (α-ADPr). (e) *In vitro* WWE-PARP14 MARylation assays demonstrate that PARP13 is a preferred PARP14 substrate. WWE-PARP14 was screened for MARylation activity using recombinant PARP13 and NXF1 in the presence of NAD^+. The same membrane was first imaged using a Ponceau S stain to detect total protein (bottom image) and then immunoblotted with MABE1016 to detect substrate MARylation (top image). * highlights a nonspecific band in the NXF1 prep. (f) Quantification of results shown in part e. The bar graphs depict the MARylation activity for NXF1 and PARP13 with WWE-PARP14 at 10 and 60 min (mean ± SEM, n = 3). ** represents p-value < 0.01, two-tailed Student's t test. ns = not significant.

PARP14 and treated with 100 μM 5-Bn-6-a-NAD^+, we observed MARylation of several protein targets across the molecular weight spectrum (Figure 1a). Importantly, this MARylation is not detected in lysates from untransfected cells or cells transfected with wild-type PARP14 (WT-ΔN-PARP14). The banding pattern produced by LG-ΔN-PARP14 is distinct from that produced by the previously characterized PARP10 variant, IG-PARP10,[18] which highlights our ability to detect mono-PARP specific protein targets. When we introduced the LG variant into the full-length PARP14 construct and performed LC-MS/MS analysis with the enriched MARylation targets, we identified 305 novel PARP14 protein targets (Supporting Table 1).

One of the main challenges when using our chemical genetics method is determining which of the PARP targets are physiologically relevant and which are false positives. Herein we describe a modification to our workflow that addresses this ambiguity. Based on a method for identifying proximal protein interactions in cells termed BioID,[21] we designed a variant of PARP14 that is fused at the N-terminus to a promiscuous form of a biotin ligase (Myc-BirA*−PARP14). When cells are treated with media containing exogenous biotin, BirA* will biotinylate nearby proteins in a diffusion-limited process allowing for identification of proximal proteins using biotin affinity capture. We expressed Myc-BirA*−PARP14 in HEK 293T cells treated with biotin, and we observed a concomitant increase in biotinylated proteins (Figure 1b). These biotinylated proteins are either interacting with PARP14 or are in close proximity to PARP14 in the cell. We then used biotin affinity capture and LC-MS/MS to identify these PARP14 "interactors". We identified 301 proteins that are selectively biotinylated in the presence of Myc-BirA*−PARP14 (Supporting Table 2).

By comparing our proteomic data sets of PARP14 MARylation targets and PARP14 "interactors", we discovered a subset of 114 proteins that are both labeled by PARP14 and spatially near PARP14 in the cell (Figure 1c). These 114 proteins represent the first global set of PARP14 targets identified in a cellular context. They now provide a new avenue for investigating the molecular function of PARP14-specific

DOI: 10.1021/acschembio.8b00567
ACS Chem. Biol. XXXX, XXX, XXX−XXX

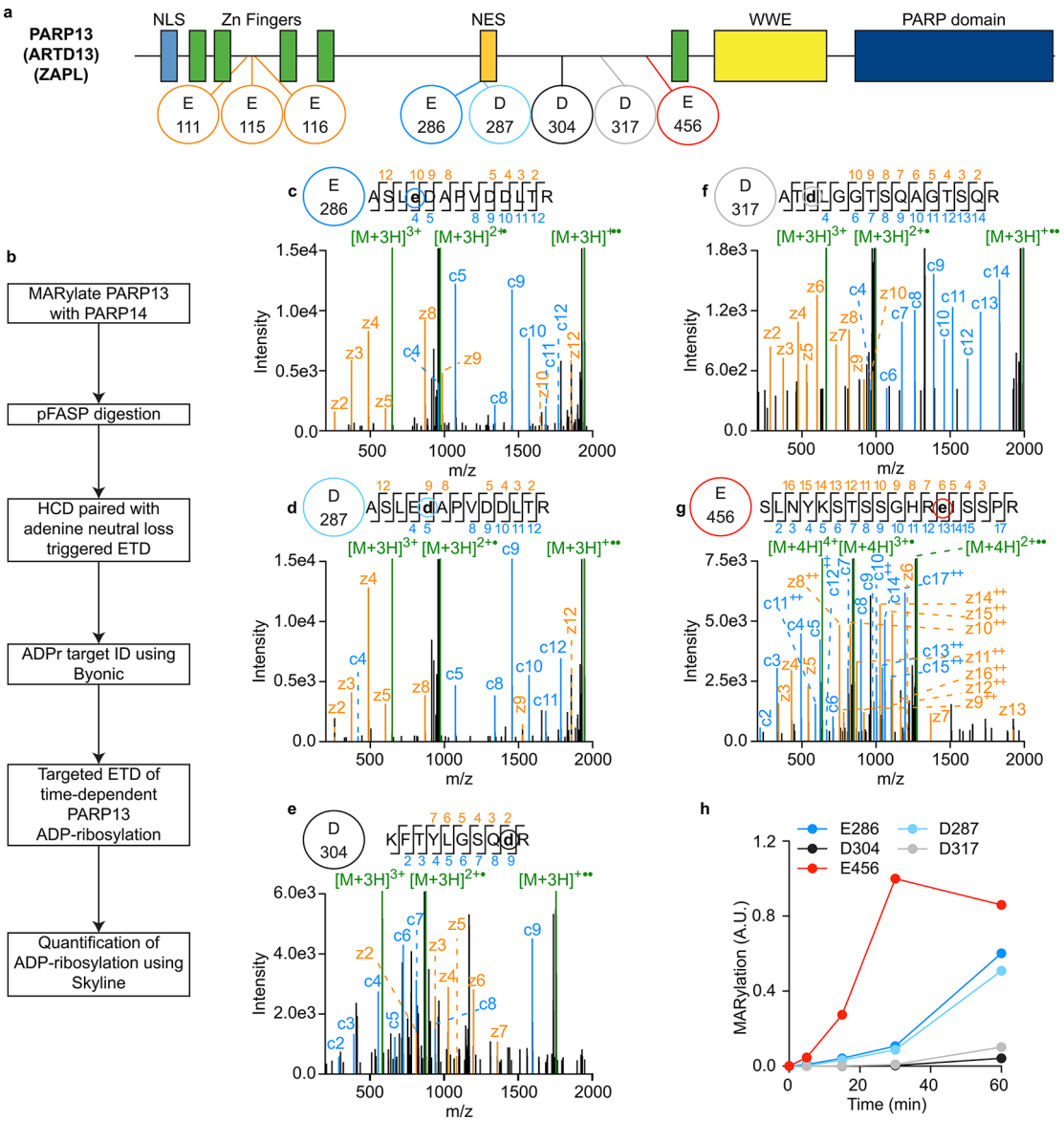

Figure 3. Identification of PARP14 MARylation sites on PARP13. (a) Domain architecture of the PARP13 protein. Amino acids that were identified as MARylation sites are indicated (orange, E111, E115, E116; blue, E286; cyan, D287; black, D304; gray, D317, and red, E456). (b) Tandem LC-MS/MS pipeline used to identify PARP13 MARylation sites. (c−g) Annotated ETD spectra for the PARP13 MARylation sites identified in the present study. Shown are representative spectra. Each peptide containing the ADPr modification is listed above the spectra, and the site of modification is indicated in bold. Coloring is the same as in part a. (h) MARylation activity for each PARP13 modification site was monitored via ETD at 5, 15, 30, and 60 min. MARylation site precursor ion intensities were normalized against the unmodified SLNYKSTSSGHREISSPR peptide. Peak integrations were performed using the sum of the peptide precursors in Skyline.

MARylation. To ascertain what roles these protein targets fulfill in the cell, we subjected them to genome ontology (GO) analysis using AmiGO (Figure 1d and Supporting Table 4).[22] We found significant enrichment for two broad subsets of biological processes: translational initiation (p-value, 6.4×10^{-20}) and SRP-dependent cotranslational targeting to membrane (p-value, 1.9×10^{-15}). Within the first category, we find enrichment for terms related to global RNA processing (e.g., RNA processing, mRNA metabolic process, post-transcriptional regulation of gene expression), which corroborates previous reports that showed a role for PARP14 in the regulation of RNA.[5,23] This GO analysis, combined with our identification of multiple RNA binding and regulatory proteins as PARP14-dependent MARylation targets, suggests that PARP14 plays a broader role in post-transcriptional regulation than previously thought.

From our chemical genetics experiments, we discovered that DEAD-box helicase 6 (DDX6) was a potential PARP14 target in the cell. While DDX6 did not pass our thresholds for being both a PARP14 target and PARP14 interactor, we thought it might still serve as a useful marker for PARP14 localization in the cell. DDX6 is involved in a range of RNA regulation activities in the cell and has been validated as a key component of post-transcriptional repression within p-bodies.[24,25] We found that GFP−PARP14 colocalized with endogenous DDX6 (Figure 2a). This colocalization occurs independently of any applied stress (e.g., sodium arsenite) or induced stress granule formation. Unlike other PARP family members, such as PARP12 and PARP13,[5] PARP14 does not localize to stress

DOI: 10.1021/acschembio.8b00567
ACS Chem. Biol. XXXX, XXX, XXX−XXX

granules (identified with the stress granules marker TIAR[26]) induced by either sodium arsenite or carbonyl cyanide-4-(trifluoromethoxy) phenylhydrazone (FCCP) (Figure S1). Together, these results show that PARP14 localizes to p-bodies and not stress granules, supporting our proteomics studies that suggest that PARP14 plays a role in post-transcriptional regulation.

After validating the formation of PARP14 positive p-bodies, we turned our attention to another intriguing PARP14 target, PARP13. PARP13 is an inactive member[27] of the PARP family and is known to play important roles in antiviral RNA repression[28] and cellular RNA regulation.[29] Here we find that PARP14 and PARP13 colocalize in HEK 293T cells in distinct subcellular puncta (Figure 2b). Interestingly, we find that the coexpression of PARP14 with PARP13 dramatically increases the surface area of the PARP14 positive puncta that we previously observed in non-PARP13 expressing cells (Figure 2c). Therefore, PARP13 appears to not only bind PARP14 in the cell but dictate the subcellular localization of PARP14 to PARP13 positive puncta. As with DDX6, these results place PARP14 inside puncta with RNA regulatory machinery and provide further evidence that PARP14 plays a role in MARylating RNA regulators in the cell.

Next, we wanted to determine if PARP14 interacts with PARP13 and if this interaction is dependent on PARP14 catalytic activity. We coexpressed HA−PARP13 and GFP−PARP14 in HEK 293T cells and pulled down PARP14 from the resulting lysate. We found that PARP13 co-immunoprecipitated with PARP14 (Figure 2d). This interaction does not depend on the addition of NAD^+ to the lysate. By treating the cells with ABT-888, a known PARP1/2-selective inhibitor,[30] we also confirmed that this interaction is independent of PARP1/2 activity. Using a catalytically inactive variant of PARP14 (GFP−PARP14-CD), we further verified that this interaction was independent of PARP14 activity. Further, the interaction between PARP14 and PARP13 is not mediated directly through RNA, as the addition of RNase A during co-immunoprecipitation had no effect on the ability of PARP14 to bind and precipitate PARP13 (Figure S2). Taken together, these results confirm that PARP14 and PARP13 share a protein−protein interaction that is both RNA and NAD^+ independent.

Our chemical genetic results demonstrated that PARP13 is MARylated by PARP14. We next sought to confirm these results using native NAD^+ as a substrate. We purified recombinant full-length PARP13 and a truncated form of PARP14 (WWE-PARP14) and assayed *in vitro* WWE-PARP14 MARylation activity. We found that WWE-PARP14 MARylates PARP13 robustly within minutes (Figure 2e). To confirm that PARP14 specifically MARylates PARP13, we compared WWE-PARP14 activity with NXF1, a previously identified PARP11 specific substrate.[18] We were surprised to find that while PARP14 significantly prefers PARP13 to NXF1 over a short time span, both substrates were modified to similar levels within an hour (Figures 2e,f). These results confirm that PARP13 is a specific PARP14 target and demonstrate that care must be taken when assaying potential PARP targets *in vitro*, as their apparent promiscuity can lead to false positive target identifications.

Lastly, we sought to identify the amino acid sites on PARP13 that are MARylated by PARP14. Previous studies have shown that PARPs can auto-MARylate on several amino acids, including glutamate and aspartate, serine, arginine, lysine, and cysteine.[31] To date, efforts to identify mono-PARP family member specific MARylation sites on target proteins have been stymied by a lack of validated specific targets. Building on the work from the Matic lab,[20] we adapted a method for identifying PARP13 MARylation sites using tandem mass spectrometry. Briefly, this method uses a combination of HCD and ETD fragmentation events. The HCD fragmentation is first used to identify peptides that undergo a neutral loss of adenosine or adenosine containing fragments. Once a peptide with an adenosine neutral loss event is detected, an ETD scan is triggered allowing for precise localization of the MARylation modification without causing the ADP-ribose moiety to be lost during fragmentation. Using this method, we identified 13 distinct PARP13 peptides that were modified by ADP-ribose when PARP13 was co-incubated with WWE-PARP14 for 1 h (Supporting Table 5). However, we had trouble confirming the exact location of the ADP-ribose signature within a peptide containing multiple potential modification sites (i.e., E, D, K, R, S, T). To address this difficulty, we created a new ETD method that searched through an inclusion list that contained only the previously identified potential PARP13 modification sites. The increase in resolution achieved with this modified ETD method allowed us to confidently assign 8 PARP13 MARylation sites (Figure 3a and Supporting Table 6). Each MS/MS spectra was manually validated to confirm the correct localization of the ADP-ribose moiety. While we allowed our search to include basic residues (K and R), cysteine, serine, and threonine, we were only able to validate acidic residues (D and E) as the sites for PARP14 modification.

Based on our *in vitro* results with both PARP13 and NFX1, we were concerned that while our 1 h time-point could reveal PARP13 sites that could be modified by PARP14, we needed a better understanding for how PARP14 targeting evolves over time. Therefore, after finding the 8 sites from the longer time point, we determined if they were differentially labeled by PARP14 or if they were modified in a stochastic manner. To answer this question we started by MARylating PARP13 with WWE-PARP14 and removed aliquots of labeled protein for site identification LC-MS/MS at regularly timed intervals (Figure 3b). During our time course, we were only able to obtain useful chromatographic information for 5 of the 8 previously identified PARP13 sites (Figure 3a). The MS/MS spectra for each of these sites were manually validated to obtain a list of key MS1 and MS2 ion signatures that would allow us to localize each ADP-ribose modification (Figures 3c−g). We used this ion list to accurately assign chromatographic peaks in the LC-MS/MS data for each site. Using Skyline,[32] a freely available reaction monitoring (SRM) client, we compiled each of the separate timed PARP13 ETD runs into a library containing the chromatographic peaks for each modified site at each time point. By integrating the peaks (see Methods for details) for each of the PARP13 MARylation sites, we could compare the respective PARP14 modification rates (Figure 3h). While we cannot rule out that the overall abundance of these sites in our LC-MS/MS data could be affected by differences in how the peptides fly during ETD fragmentation, we still notice a stark difference in the rates at which PARP14 modifies the different PARP13 sites. Roughly, these sites can be broken into three categories: fast (E456), moderate (E286 and D287), and slow (D304 and D317). This provides the first evidence that mono-PARPs display a site-specific preference on the same target protein and that the

DOI: 10.1021/acschembio.8b00567
ACS Chem. Biol. XXXX, XXX, XXX−XXX

catalytic domain alone is capable of distinguishing between these sites.

To confirm our site identification LC-MS/MS results, we introduced a series of point mutations into recombinant PARP13 and subjected the variants to *in vitro* ADP-ribosylation using WWE-PARP14. Surprisingly, we found that mutation of the "fast" site to an alanine residue (PARP13-E456A) resulted in more labeling at both 10 and 60 min as compared to the WT construct (Figure 4a,b). Based

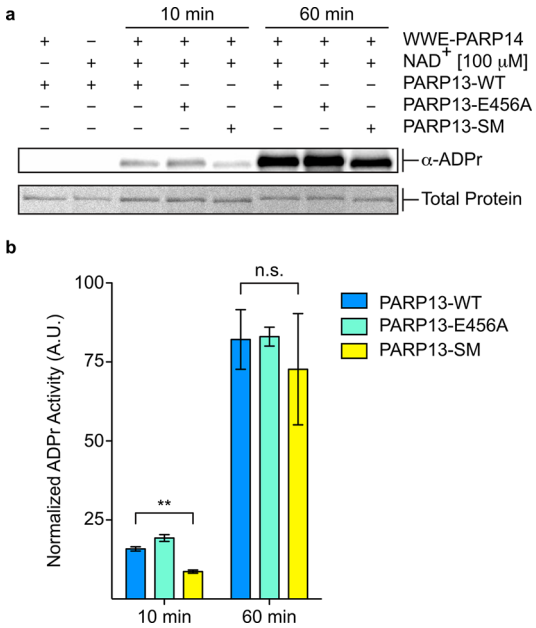

Figure 4. *In vitro* validation of specific PARP13 MARylation sites using WWE-PARP14 and NAD$^+$. (a) WWE-PARP14 was screened for MARylation activity using recombinant PARP13 variants in the presence of NAD$^+$. The same membrane was first imaged using a Ponceau S stain to detect total protein (bottom image) and then immunoblotted with MABE1016 to detect substrate MARylation (top image). (b) Quantification of results shown in part a. The bar graphs depict the MARylation activity for the PARP13 variants with WWE-PARP14 at 10 and 60 min (mean ± SEM, n = 3). ** represents p-value < 0.01, two-tailed Student's t test. ns = not significant.

on these results, it is possible that the E456 site plays an inhibitory role and blocks modification of additional sites within PARP13. Further, it is possible that the mutation we introduced could alter the PARP13 structure and reveal new modification sites. Regardless, when we mutate all of the 8 sites we identified to alanine (PARP13-SM) we see a significant reduction in PARP14-dependent labeling (~50% of WT labeling) at 10 min and a nonsignificant reduction after an hour (Figure 4b). The inability to drive PARP14-dependent MARylation to zero could indicate that there are additional sites we have not accounted for, that the WWE-PARP14 construct does not reproduce fully the preferences of the full-length cellular PARP14, or that PARP14 can modify additional glutamates and aspartates to compensate for the loss of its preferred sites. To rule out significant structural changes in PARP13 that might be caused by our mutations, we compared the ability of the WT and SM variant to bind a previously characterized PARP13-bound RNA fragment.[29] Both the WT and SM variant bound RNA with a similar K_d (118.8 nM vs 127.6 nM, respectively) suggesting that our mutations did not radically alter the structure of PARP13 (Figure S3). Taken together, we have demonstrated that PARP14 modifies PARP13, we have identified a series of PARP13 sites that are specifically MARylated by PARP14, and we have confirmed that our mutations do not effect RNA binding functions of PARP13.

In summary, we used our chemical genetics strategy together with a BioID proximity labeling approach to identify direct targets of PARP14. We found that PARP14 specifically MARylates and interacts with a number of diverse RNA regulatory proteins and is localized with DDX6 to RNA p-bodies. Further, we identified another PARP family member, PARP13, as a bona fide PARP14 MARylation target. In addition, we were able to identify and validate a number of new PARP14-dependent MARylation sites on PARP13. Using our pipeline, it is now possible to go from a specific PARP family member to its direct targets and from there to the exact sites of modification.

Our identification of individual PARP13 MARylation sites presents a number of intriguing questions for future study. In particular, we are interested in uncovering whether the MARylation sites are involved in RNA recognition or regulation events, if they play a role in antiviral repression, or if they are important for an as-yet unknown PARP13 function. As the validated biological roles for the PARP family, and PARP14 in particular, continue to expand, this work should aid in the elucidation of the function of MARylation in normal physiology and disease.

METHODS

Chemical Synthesis. Synthesis of 5-Bn-6-a-NAD$^+$ and 6-a-NAD$^+$ was completed as previously described.[16,18]

Cloning Full-Length PARP14. To generate full-length PARP14 constructs, PCR primers were designed to amplify the entirety of the PARP14 coding sequence flanked by various restriction enzyme sites. Amplified PARP14 was cut, gel-purified, and ligated into various expression constructs. PARP14 containing vectors were transformed into NEB Stable cells (NEB), and they were recovered at 30 °C for 1 h in LB media. Following plating, they were incubated at RT for 2 days, and resulting colonies were grown in LB/Kan media at 24 °C instead of 37 °C. Following clonal expansion, plasmids were purified using Midiprep kits (Thermo).

Cell Culture and Immunofluorescence. HEK 293T cells were grown in DMEM (Gibco) supplemented with 10% fetal bovine serum (FBS, HyClone), penicillin/streptomycin (Invitrogen), and 1× GlutaMAX (Gibco) at 37 °C and 5% CO_2. Transient transfections of HEK 293T cells with 20 μg of GFP-tagged or Myc-BirA* expression vectors per 10 cm dish (~70% confluency) were performed using the CalPhos system (Clontech) according to manufacturer's instructions. For coexpression experiments, GFP−PARP14 vectors were transfected 1:1 with HA−PARP13 or an empty vector (as a negative control). Cells were lysed in HEPES buffer supplemented with cOmplete EDTA-free protease inhibitor (Roche), and cell debris was cleared by centrifugation at 14 000g for 5 min at 4 °C. Immunofluoresence localization experiments with GFP−PARP14, DDX6, TIAR, and HA−PARP13 were performed as previously described.[18] The treatment of cells with sodium arsenite and FCCP to induce stress granule formation was based on published reports.[33] Images were collected on an ApoTome microscope (Zeiss) and were processed using ImageJ. Z-stacks were compressed as maximal 2D projections, and background subtraction was completed using the Rolling Ball Background Subtraction plugin (radius = 8).

NeutrAvidin Enrichment and LC-MS/MS Analysis. Total protein (0.5−1 mg) from HEK 293T cells expressing WT- or LG-PARP14 was incubated with 100 μM 5-Bn-6-a-NAD$^+$ for 2 h at 30 °C, click conjugated to biotin−PEG$_3$-azide, and subjected to enrichment using NeutrAvidin agarose (Pierce) and proteolysis as described.[16−18]

DOI: 10.1021/acschembio.8b00567
ACS Chem. Biol. XXXX, XXX, XXX−XXX

The labeling of Myc-BirA*−PARP14 interactors with biotin was performed as previously reported.[21] Briefly, HEK 293T cells expressing GFP−PARP14 or Myc-BirA*−PARP14 were treated with media supplemented with 50 μM biotin for 24 h prior to protein extraction. Biotinylated proteins were subjected to NeutrAvidin agarose enrichment and target identification as described.[16−18] The PARP13 MARylation site identification experiments were performed with 150 μg of recombinant PARP13 that was labeled for 30 min at 30 °C with 3 μM WWE-PARP14 and 100 μM NAD^+. MARylated PARP13 was digested via partial proteolysis with 1.5 ng/μL trypsin (Promega) for 20 min at RT and purified using filter aided sample prep (FASP) as described previously.[20] Time course experiments were completed as described above except aliquots of 150 μg of PARP13 were removed and precipitated in methanol at 5, 15, 30, or 60 min prior to LC-MS/MS sample preparation. MS experiments were performed using an Orbitrap Fusion (Thermo) equipped with a nanospray UPLC system. MS processing and analysis thresholds are discussed in Supporting Information.

PARP14 Selectivity Assay. Recombinant proteins were preceded by a 6× His tag and were expressed and purified as previously described.[16] In addition to Ni-NTA affinity chromatography, PARP13 constructs were further purified via size-exclusion chromatography using a Superdex 200 Increase 10/300 column (GE Healthcare). WWE-PARP14 (5 nM) was incubated with either PARP13 or NXF1 (500 nM) and 100 μM NAD^+ for 10 or 60 min at 30 °C in an 18 μL reaction volume consisting of 50 mM Tris-HCl, pH 7.5, 100 mM NaCl, 12 mM $MgCl_2$, and 0.5 mM TCEP. Substrate labeling was detected via immunoblot using the pan-ADP-ribose detection reagent MABE1016 (Millipore) and quantified using ImageLab v5.2 (Bio-Rad) and normalized against the total substrate load as determined using Ponceau S stain. The MARylation activity was normalized against PARP13 activity at 60 min.

PARP13 Site Validation. WWE-PARP14 (5 nM) was incubated with either PARP13-EA, the E456A point mutant (PARP13-E456A), or the E111A, E115A, E116A, E286A, D287A, D304A, D317A, and E456A mutant (PARP13-SM) (500 nM), and treated as detailed above in the PARP14 selectivity assay. The MARylation activity was normalized against PARP13-WT activity at 60 min.

■ ASSOCIATED CONTENT

Supporting Information

The Supporting Information is available free of charge on the ACS Publications website at DOI: 10.1021/acschembio.8b00567.

Target list for LG-PARP14−5-Bn-6-a-NAD^+ method, target list for BioID with Myc-BirA*−PARP14, background target list for common proteins found in control LC-MS/MS experiments with NAD^+ analogs, GO term enrichment for PARP14 targets and "interactors", PARP13 sites identified using mixed HCD-ETD fragmentation, and PARP13 sites identified using ETD fragmentation with an inclusion list (XLSX)

PARP14 localization separate from stress granules, coprecipitation of HA−PARP13 and GFP−PARP14, PARP13 binding of 3′UTR of TRAILR4, supporting experimental procedures, and expanded methods for MS/MS acquisition and processing (PDF)

■ AUTHOR INFORMATION

Corresponding Authors

*cohenmic@ohsu.edu.

*icarteroconnell@scu.edu.

ORCID

Ian Carter-O'Connell: 0000-0002-2344-3483

Rory K. Morgan: 0000-0003-0194-0304

Michael S. Cohen: 0000-0002-7636-4156

Present Address

§I.C.-O.: Department of Chemistry and Biochemistry, Santa Clara University, Santa Clara, CA 95053, United States.

Notes

The authors declare no competing financial interest.

Raw and processed MS data files are available at www.peptideatlas.org (ID: PASS01067).

■ ACKNOWLEDGMENTS

We thank J. Klimek for assistance with the MS analysis at the OHSU proteomics core, M. Levinson for assistance with reagent preparation, I. Kirby for the recombinant WWE-PARP14 protein, and P. Chang for the GFP−PARP14 construct. We thank members of the Cohen lab for many helpful discussions regarding the manuscript and experimental design. This work was funded by the National Institutes of Health (NIH 1R01NS088629) to M.S.C., and I.C.-O. was supported by a Postdoctoral Fellowship (PF-15-008-01-CDD) from the American Cancer Society. This work was also supported by the following NIH grants: he following NIH grants: S10 OD012246, P30 EY010572, and P30 CA069533. The authors declare no competing financial interests.

■ REFERENCES

(1) Hottiger, M. O., Hassa, P. O., Lüscher, B., Schüler, H., and Koch-Nolte, F. (2010) Toward a Unified Nomenclature for Mammalian ADP-Ribosyltransferases. *Trends Biochem. Sci. 35*, 208−219.

(2) Kashima, L., Idogawa, M., Mita, H., Shitashige, M., Yamada, T., Ogi, K., Suzuki, H., Toyota, M., Ariga, H., Sasaki, Y., and Tokino, T. (2012) CHFR Protein Regulates Mitotic Checkpoint by Targeting PARP-1 Protein for Ubiquitination and Degradation. *J. Biol. Chem. 287*, 12975−12984.

(3) Anjos, S. M., Robert, R., Waller, D., Zhang, D. L., Balghi, H., Sampson, H. M., Ciciriello, F., Lesimple, P., Carlile, G. W., Goepp, J., Liao, J., Ferraro, P., Dantzer, F., Hanrahan, J. W., Thomas, D. Y., and Phillipe, R. (2012) Decreasing Poly(ADP-Ribose) Polymerase Activity Restores ΔF508 CFTR Trafficking. *Front. Pharmacol. 3*, 165.

(4) Goldberg, S., Visochek, L., Giladi, E., Gozes, I., and Cohen-Armon, M. (2009) PolyADP-Ribosylation Is Required for Long-Term Memory Formation in Mammals. *J. Neurochem. 111*, 72−79.

(5) Leung, A. K. L., Vyas, S., Rood, J. E., Bhutkar, A., Sharp, P. A., and Chang, P. (2011) Poly(ADP-Ribose) Regulates Stress Responses and MicroRNA Activity in the Cytoplasm. *Mol. Cell 42*, 489−499.

(6) Gibson, B. A., and Kraus, W. L. (2012) New Insights into the Molecular and Cellular Functions of Poly(ADP-Ribose) and PARPs. *Nat. Rev. Mol. Cell Biol. 13*, 411−424.

(7) Vyas, S., Matic, I., Uchima, L., Rood, J., Zaja, R., Hay, R. T., Ahel, I., and Chang, P. (2014) Family-Wide Analysis of Poly(ADP-Ribose) Polymerase Activity. *Nat. Commun. 5*, 4426.

(8) Ruf, A., Rolli, V., de Murcia, G., and Schulz, G. E. (1998) The Mechanism of the Elongation and Branching Reaction of Poly(ADP-Ribose) Polymerase as Derived from Crystal Structures and Mutagenesis. *J. Mol. Biol. 278*, 57−65.

(9) Hassa, P. O., and Hottiger, M. O. (2008) The Diverse Biological Roles of Mammalian PARPS, a Small but Powerful Family of Poly-ADP-Ribose Polymerases. *Front. Biosci., Landmark Ed. 13*, 3046−3082.

(10) Goenka, S., and Boothby, M. (2006) Selective Potentiation of Stat-Dependent Gene Expression by Collaborator of Stat6 (CoaSt6), a Transcriptional Cofactor. *Proc. Natl. Acad. Sci. U. S. A. 103*, 4210−4215.

(11) Goenka, S., Cho, S. H., and Boothby, M. (2007) Collaborator of Stat6 (CoaSt6)-Associated Poly(ADP-Ribose) Polymerase Activity

DOI: 10.1021/acschembio.8b00567
ACS Chem. Biol. XXXX, XXX, XXX−XXX

Modulates Stat6-Dependent Gene Transcription. *J. Biol. Chem. 282*, 18732−18739.

(12) Cho, S. H., Raybuck, A., Wei, M., Erickson, J., Nam, K. T., Cox, R. G., Trochtenberg, A., Thomas, J. W., Williams, J., and Boothby, M. (2013) B Cell-Intrinsic and -Extrinsic Regulation of Antibody Responses by PARP14, an Intracellular (ADP-Ribosyl)Transferase. *J. Immunol. 191*, 3169−3178.

(13) Caprara, G., Prosperini, E., Piccolo, V., Sigismondo, G., Melacarne, A., Cuomo, A., Boothby, M., Rescigno, M., Bonaldi, T., and Natoli, G. (2018) PARP14 Controls the Nuclear Accumulation of a Subset of Type I IFN-Inducible Proteins. *J. Immunol. 200*, 2439−2454.

(14) Barbarulo, A., Iansante, V., Chaidos, A., Naresh, K., Rahemtulla, A., Franzoso, G., Karadimitris, A., Haskard, D. O., Papa, S., and Bubici, C. (2013) Poly(ADP-Ribose) Polymerase Family Member 14 (PARP14) Is a Novel Effector of the JNK2-Dependent pro-Survival Signal in Multiple Myeloma. *Oncogene 32*, 4231−4242.

(15) Iansante, V., Choy, P. M., Fung, S. W., Liu, Y., Chai, J.-G., Dyson, J., Del Rio, A., D'Santos, C., Williams, R., Chokshi, S., Anders, R. A., Bubici, C., and Papa, S. (2015) PARP14 Promotes the Warburg Effect in Hepatocellular Carcinoma by Inhibiting JNK1-Dependent PKM2 Phosphorylation and Activation. *Nat. Commun. 6*, 7882.

(16) Carter-O'Connell, I., Jin, H., Morgan, R. K., David, L. L., and Cohen, M. S. (2014) Engineering the Substrate Specificity of ADP-Ribosyltransferases for Identifying Direct Protein Targets. *J. Am. Chem. Soc. 136*, 5201−5204.

(17) Carter-O'Connell, I., and Cohen, M. S. (2015) Identifying Direct Protein Targets of Poly-ADP-Ribose Polymerases (PARPs) Using Engineered PARP Variants-Orthogonal Nicotinamide Adenine Dinucleotide (NAD+) Analog Pairs. *Curr. Protoc. Chem. Biol. 7*, 121−139.

(18) Carter-O'Connell, I., Jin, H., Morgan, R. K., Zaja, R., David, L. L., Ahel, I., and Cohen, M. S. (2016) Identifying Family-Member-Specific Targets of Mono-ARTDs by Using a Chemical Genetics Approach. *Cell Rep. 14*, 621−631.

(19) Gibson, B. A., Zhang, Y., Jiang, H., Hussey, K. M., Shrimp, J. H., Lin, H., Schwede, F., Yu, Y., and Kraus, W. L. (2016) Chemical Genetic Discovery of PARP Targets Reveals a Role for PARP-1 in Transcription Elongation. *Science 353*, 45−50.

(20) Leidecker, O., Bonfiglio, J. J., Colby, T., Zhang, Q., Atanassov, I., Zaja, R., Palazzo, L., Stockum, A., Ahel, I., and Matic, I. (2016) Serine Is a New Target Residue for Endogenous ADP-Ribosylation on Histones. *Nat. Chem. Biol. 12* (12), 998−1000.

(21) Roux, K. J., Kim, D. I., and Burke, B. (2013) BioID: A Screen for Protein-Protein Interactions. *Curr. Protoc. Protein Sci. 74*, 19.23.1.

(22) Carbon, S., Ireland, A., Mungall, C. J., Shu, S., Marshall, B., Lewis, S., AmiGO Hub, and Web Presence Working Group (2009) AmiGO: Online Access to Ontology and Annotation Data. *Bioinformatics 25*, 288−289.

(23) Iqbal, M. B., Johns, M., Cao, J., Liu, Y., Yu, S.-C., Hyde, G. D., Laffan, M. A., Marchese, F. P., Cho, S. H., Clark, A. R., Gavins, F. N., Woollard, K. J., Blackshear, P. J., Mackman, N., Dean, J. L., Boothby, M., and Haskard, D. O. (2014) PARP-14 Combines with Tristetraprolin in the Selective Posttranscriptional Control of Macrophage Tissue Factor Expression. *Blood 124*, 3646−3655.

(24) Minshall, N., Kress, M., Weil, D., and Standart, N. (2009) Role of P54 RNA Helicase Activity and Its C-Terminal Domain in Translational Repression, P-Body Localization and Assembly. *Mol. Biol. Cell 20*, 2464−2472.

(25) Serman, A., Le Roy, F., Aigueperse, C., Kress, M., Dautry, F., and Weil, D. (2007) GW Body Disassembly Triggered by SiRNAs Independently of Their Silencing Activity. *Nucleic Acids Res. 35*, 4715−4727.

(26) Kedersha, N. L., Gupta, M., Li, W., Miller, I., and Anderson, P. (1999) RNA-Binding Proteins TIA-1 and TIAR Link the Phosphorylation of EIF-2 Alpha to the Assembly of Mammalian Stress Granules. *J. Cell Biol. 147*, 1431−1442.

(27) Karlberg, T., Klepsch, M., Thorsell, A.-G., Andersson, C. D., Linusson, A., and Schüler, H. (2015) Structural Basis for Lack of ADP-Ribosyltransferase Activity in Poly(ADP-Ribose) Polymerase-13/Zinc Finger Antiviral Protein. *J. Biol. Chem. 290*, 7336−7344.

(28) Gao, G., Guo, X., and Goff, S. P. (2002) Inhibition of Retroviral RNA Production by ZAP, a CCCH-Type Zinc Finger Protein. *Science 297*, 1703−1706.

(29) Todorova, T., Bock, F. J., and Chang, P. (2014) PARP13 Regulates Cellular MRNA Post-Transcriptionally and Functions as a pro-Apoptotic Factor by Destabilizing TRAILR4 Transcript. *Nat. Commun. 5*, 5362.

(30) Donawho, C. K., Luo, Y., Luo, Y., Penning, T. D., Bauch, J. L., Bouska, J. J., Bontcheva-Diaz, V. D., Cox, B. F., DeWeese, T. L., Dillehay, L. E., et al. (2007) ABT-888, an Orally Active Poly(ADP-Ribose) Polymerase Inhibitor That Potentiates DNA-Damaging Agents in Preclinical Tumor Models. *Clin. Cancer Res. 13*, 2728−2737.

(31) Cohen, M. S., and Chang, P. (2018) Insights into the Biogenesis, Function, and Regulation of ADP-Ribosylation. *Nat. Chem. Biol. 14*, 236−243.

(32) MacLean, B., Tomazela, D. M., Shulman, N., Chambers, M., Finney, G. L., Frewen, B., Kern, R., Tabb, D. L., Liebler, D. C., and MacCoss, M. J. (2010) Skyline: An Open Source Document Editor for Creating and Analyzing Targeted Proteomics Experiments. *Bioinformatics 26*, 966−968.

(33) Ruggieri, A., Dazert, E., Metz, P., Hofmann, S., Bergeest, J.-P., Mazur, J., Bankhead, P., Hiet, M.-S., Kallis, S., Alvisi, G., et al. (2012) Dynamic Oscillation of Translation and Stress Granule Formation Mark the Cellular Response to Virus Infection. *Cell Host Microbe 12*, 71−85.

DOI: 10.1021/acschembio.8b00567
ACS Chem. Biol. XXXX, XXX, XXX−XXX